

# Closing the Sim2Real Gap in Dynamic Cloth Manipulation

Julius Hietala, David Blanco-Mulero, Gokhan Alcan, Ville Kyrki

**Abstract**— Cloth manipulation is a challenging task due to the many degrees of freedom and properties of the material affecting the dynamics of the cloth. The nonlinear dynamics of the cloth have particularly strong significance in dynamic cloth manipulation, where some parts of the cloth are not directly controllable. In this paper, we present a novel approach for solving dynamic cloth manipulation by training policies using reinforcement learning (RL) in simulation and transferring the learned policies to the real world in a zero-shot manner. The proposed method uses visual feedback and material property randomization in a physics simulator to achieve generalization in the real world. Experimental results show that using only visual feedback is enough for the policies to learn the dynamic manipulation task in a way that transfers from simulation to the real world. In addition, the randomization of the dynamics in simulation enables capturing the behavior of a variety of cloths in the real world.

## I. INTRODUCTION

Research on cloth manipulation has gained increasing interest over the past years since it has many potential real world applications from bed-making to folding cloths. However, when compared to manipulation of rigid objects, manipulating deformable objects such as cloth presents a different set of challenges. Cloths have infinite degrees of freedom whereas rigid objects have only a few. For rigid objects, knowing their position and orientation is usually enough to describe their location in the world. For deformable objects such a simple representation is not available, which forces to come up with more complex representations depending on the application. Any cloth manipulation approach requiring information about the location of the cloth must thus infer the information implicitly from images, or use some simplification, such as only tracking a few points for which estimates of the position and orientation can be made.

Even though we are still far away from industry-grade solutions for general bed making, cloth folding, and other everyday tasks involving fabrics, many interesting solutions for folding and flattening cloths in the real world have been proposed ([1], [2], [3], [4]). A common denominator of these solutions is that they only involve static or quasi-static manipulation [5], thus limiting the range of tasks that can be performed.

In this paper, we focus on dynamic manipulation [5] of cloths in the real world using a single robotic arm. In addition to kinematics, static and quasi-static forces, dynamic

This work was financially supported by Academy of Finland grant numbers 328399 and 317020.

All authors are with Intelligent Robotics Group, Department of Electrical Engineering and Automation (EEA), Aalto University, Espoo, Finland. [{julius.hietala, david.blancomulero, gokhan.alcan, ville.kyrki}@aalto.fi](mailto:{julius.hietala, david.blancomulero, gokhan.alcan, ville.kyrki}@aalto.fi)

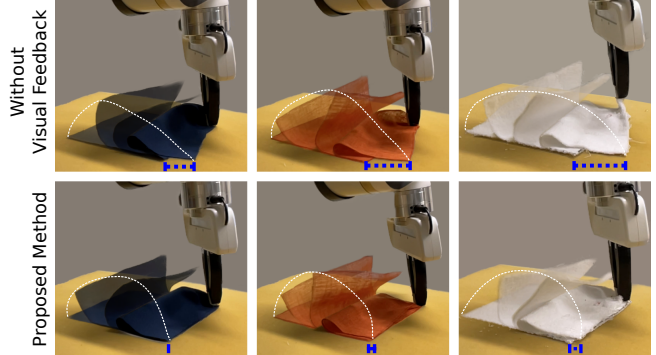


Fig. 1: The proposed method performs well in a dynamic cloth manipulation task for different types of fabrics when compared to a fixed trajectory from a policy trained in simulation without visual feedback. The dashed blue line indicates the distance from the end position of the cloth non-controlled point to the target point.

manipulation involves forces caused by the acceleration of the manipulator and consequently the manipulated fabric. These forces increase the difficulty of manipulation tasks, but allow manipulating parts of the fabric that are not grasped. This opens a new avenue of tasks compared to tasks where only the grasped part of the fabric is manipulated. In general, dynamic cloth manipulation presents the following challenges:

- Observing the position and velocity of the cloth is not trivial. Cloth manipulation methods need to either observe the cloth visually [6] or use a motion capture system with markers attached to the cloth [7]. In dynamic manipulation, observing the velocity is especially important since the task success depends on forces caused by acceleration.
- The behavior of the cloth is dependent on its material properties. A fixed trajectory that successfully manipulates a certain cloth to a desired configuration does not necessarily achieve the same configuration on a different type of fabric (see Fig. 1).
- Commanding the robot to achieve the dynamic manipulation motions is not straightforward. Static manipulation can often be achieved by only getting the robot to follow a desired path, whereas dynamic manipulation also requires determining appropriate velocities through the path’s way-points, which is challenging especially if the trajectory is determined step by step based on visual feedback. Prior work in dynamic cloth manipulation has solved this by allowing free arbitrary Cartesian 3D

motion (only feasible in simulation) [8] or by using limited predefined dynamic action primitives [9].

In order to achieve dynamic cloth manipulation in the real world and solve the aforementioned challenges, we propose a method that uses Reinforcement Learning (RL) to train policies that learn to achieve dynamic cloth manipulation based on visual feedback. In Fig. 1, we show qualitative results of the proposed method compared to a method without visual feedback. The trained policies learn to account for different cloth dynamics and use a task-agnostic Cartesian controller to achieve the desired dynamic manipulation. The policies are trained using data from simulation and transferred to the real world in a zero-shot manner. The main contributions of our work are:

- 1) This is the first work to perform dynamic cloth manipulation using visual feedback and task-agnostic actions in the real world. The proposed method is able to transfer policies without a need for fine-tuning the domain shift between the simulated and the real world environments.
- 2) We solve the challenge of adapting a policy to different fabrics by combining visual feedback and domain randomization of the simulated cloth dynamics. We show that randomizing cloth parameters in simulation helps the trained policies generalize across a range of material types in the real world instead of a single material.
- 3) We combine the RL policy with a Cartesian controller in the policy learning process enabling the dynamic motions required by dynamic cloth manipulation.

The organization of this paper is as follows. Section II discusses related work in cloth manipulation. The cloth manipulation reinforcement learning problem is formulated in Section III. Section IV starts with an overview of the proposed method, followed by the strategy to learn policies in simulation and the methods used to close the Sim2Real gap. We define a dynamic sideways folding task as well as the experimental setup, and discuss the results in Section V and Section VI respectively. Finally, the paper is concluded with some remarks and future work in Section VII.

## II. RELATED WORK

Robotic manipulation of deformable objects such as cloth has been studied extensively in various contexts including getting dressed ([3], [4]), laundry folding [10], and bed-making [2]. Many of the methods rely on observing features such as corners, edges, and wrinkles of the cloths ([11], [2], [10], [12], [11], [13], [14]) and then performing manipulation actions via a learning method or heuristic. In contrast, methods presented by [6], [15], [16], [9], [17] determine manipulation actions directly from visual observations without intermediate feature extraction for downstream use.

The majority of the work in cloth manipulation make use of engineered action primitives, most commonly sequential pick-and-place actions [15], [18], [2], which are easier to program and execute on real robots compared to a free

Cartesian motion. In contrast, both [8] and [6] define the action spaces as a 3D desired Cartesian velocity and a boolean grasp action. Performing such Cartesian motion is challenging in the real world, but since the tasks considered in [6] are only quasi-static, the authors are able to command the real robot using inverse kinematics and a joint velocity controller. Jangir *et al.* [8] also perform tasks requiring dynamic manipulation, but only do so in simulation where the end-effector can move arbitrarily in the 3D space. To our knowledge, dynamic cloth manipulation in the real world using visual feedback has only been performed by Ha *et al.* [9] where they concentrate purely on cloth unfolding. However, their set of actions is limited to a set of predefined dynamic movement primitives, where only the grasp locations are parameterized, vastly simplifying the real world implementation.

The current state of the art in dynamic cloth folding is limited to folding in simulation and a single type of fabric. The method presented by Jangir *et al.* [8] also relies on the exact position and velocity information of the cloth points and the free Cartesian 3D motion of the manipulator, which both are infeasible to implement directly in the real world. Thus, their methodology can only be executed in the real world by training a policy in simulation and collecting a successful trajectory, which then can be executed on real hardware without any feedback.

## III. PROBLEM STATEMENT

The problem we consider is an RL problem where a robotic manipulator interacts in finite episodes over discrete time steps with a cloth that needs to be manipulated to a goal configuration following a policy. The internal state of the cloth cannot be observed in the real world. Instead, we can only partially observe its state from visual feedback. Therefore, we formulate the dynamic cloth manipulation problem as a Partially Observable Markov Decision Process (POMDP). The POMDP is defined as a tuple  $(S, A, O, P, R, \Omega, T, \gamma)$ , where  $S$  is the set of states,  $A$  is the set of actions that can be taken by the agent, and  $O$  is the set of partial observations. Here the partial observations  $\mathbf{o}_t \in O$  are images of the cloth, that the agent observes at each time step. The probability of observing a state is given by  $\Omega(\mathbf{o}_t, \mathbf{s}_t, \mathbf{a}_t) = p(\mathbf{o}_t \mid \mathbf{s}_t, \mathbf{a}_t)$ , and  $T(\mathbf{s}_{t+1}, \mathbf{s}_t, \mathbf{a}_t) = p(\mathbf{s}_{t+1} \mid \mathbf{s}_t, \mathbf{a}_t)$  is the transition probability from state  $\mathbf{s}_t$  to the next state  $\mathbf{s}_{t+1}$  following an action  $\mathbf{a}_t$ . In our formulation, we also include a goal  $\mathbf{g} \in G$  for the agent at each episode, which is used to determine whether the cloth manipulation task is successful or not. Thus, the reward function of an agent performing an action  $\mathbf{a}_t$  is given  $R(\mathbf{s}_t, \mathbf{a}_t, \mathbf{g})$ , where  $\gamma \in (0, 1]$  the discount factor.

The goal of the RL agent is to find the optimal policy  $\pi^*$ , parametrized by  $\theta^*$ , that maximizes the expected value of the cumulative reward

$$\pi^* = \operatorname{argmax}_{\pi} \mathbb{E} \left[ \sum_{n=1}^N \gamma^n R(\mathbf{s}_t, \mathbf{a}_t, \mathbf{g}) \right]. \quad (1)$$

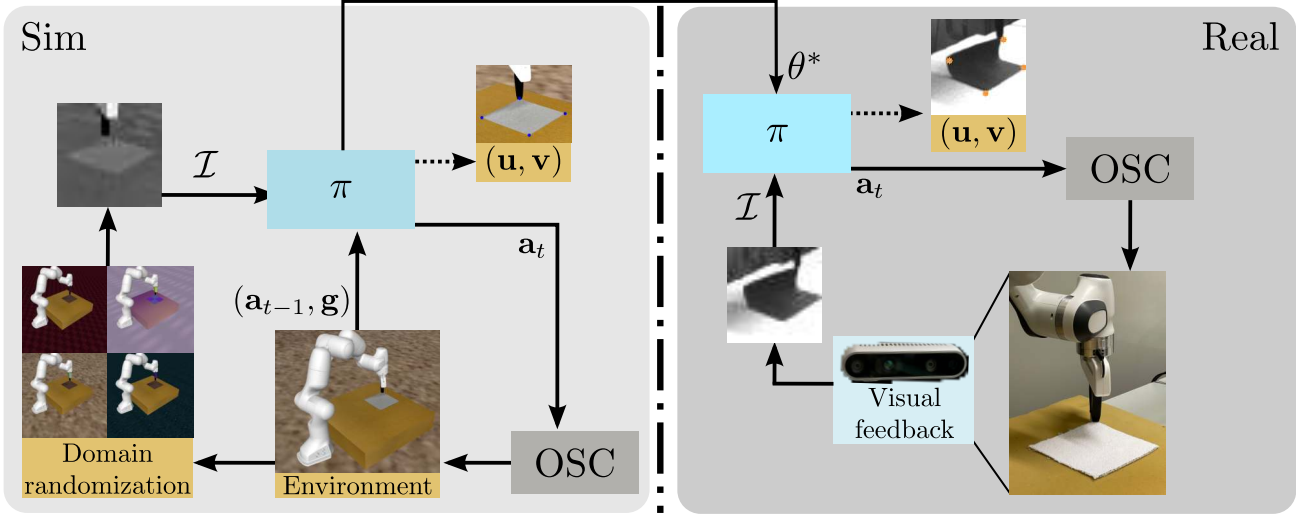


Fig. 2: Overview of the proposed cloth manipulation method. The simulation (left side) consists of an environment where the dynamics of the cloth are randomized along with the visual properties of the environment. The real world setup (right side) receives the optimal parameters  $\theta^*$  of the policies trained in simulation. The policies receive an image  $I$ , a goal  $g$  and the previous action  $a_{t-1}$  as input. The output of the policy is the next action  $a_t$  as well as a prediction of the cloth corners  $(u, v)$ . Both simulation and real setup use the same Cartesian controller, namely Operational Space Control (OSC).

#### IV. PROPOSED METHOD

A general view of our proposed method for dynamic cloth manipulation is depicted in Fig. 2. The RL policies are trained in simulation, where we perform domain randomization including multiple cloth dynamics, which is used for generalization across different fabric types. In both the sim (left side Fig. 2) and real system (right side Fig. 2) we use the same structure of visual input  $I$ , and the same Cartesian controller, Operational Space Control (OSC) [19], which facilitates transferring the policy trained in simulation in a zero-shot manner.

##### A. Learning in Simulation

In order to efficiently gather training data for policies that run in the real world, we use a physics engine simulator. The cloth is simulated as a 2D grid of bodies connected via a spring-damper system, where one of the corners is connected to the robot end-effector with a rigid link. The simulation provides the internal states  $S$  of the cloth, along with an image  $I \in O$  of the cloth. The images serve as the partial observations of the RL problem and are used by the policy  $\pi$  to determine the next action  $a_t$ . The policy also takes as input the previous action  $a_{t-1}$  and a goal  $g$  that represents the desired cloth configuration. The policy is composed of three mappings

$$\pi : \begin{cases} h_1 : I \rightarrow \mathcal{L} \\ h_2 : (\mathcal{L}, a_{t-1}, g) \rightarrow a_t \\ h_3 : \mathcal{L} \rightarrow (u, v) \end{cases} \quad (2)$$

First, the input image is mapped to a latent space  $\mathcal{L}$  via  $h_1$ . The second mapping  $h_2$  outputs the continuous action  $a_t$ , which is the desired change in the end-effector position.

The last mapping  $h_3$  provides an auxiliary output with the estimated position of cloth points  $(u, v)$  in the image plane. The first mapping is implemented as a convolutional neural network (CNN), whereas the other two mappings are fully connected neural networks.

We use Soft-Actor Critic (SAC) [20] for learning the cloth manipulation policy. Additionally, our method uses Hindsight Experience Replay (HER) [21] to speed up training, and 10% of trajectories added to the replay buffer are real world demonstrations with added Gaussian noise in the action  $a_t$ . In our system, the Q functions of SAC observe the position and velocity of  $C$  cloth points  $\{\mathbf{p}_i, \dot{\mathbf{p}}_i\}_{i=1}^C \in S$ , along with the goal and current action. The reason behind the observation asymmetry between the policy and the Q functions is that the cloth body position and velocity information is not available in the real world, and the Q functions are only needed during training. The fact that the policy observes only the images rather than the cloth points facilitates transferring the policy to the real world.

##### B. Closing the Sim2Real gap

In order to close the Sim2Real gap and transfer the policies in a zero-shot manner we consider two main elements: 1) domain randomization including the dynamic and visual properties of the cloth, and 2) embedding the Cartesian controller used in the real hardware into the policy learning process.

For the domain randomization process we begin by uniformly sampling cloth dynamics parameters from  $\theta_c \sim \mathcal{U}_{[a, b]}$ , where  $[a, b]$  includes empirically chosen ranges for each parameter. Then, we evaluate simulated cloths with parameters  $\theta_c$  using expert demonstrations from the real world that achieve success on the real world cloth manipulation

task (see Section V-A). Out of the tested cloths, the top  $M$  sets of parameters that achieve the highest reward at the end of an episode are picked, giving us the set of simulated cloths  $F_{sim} = \{f_1, \dots, f_M\}$ . We use  $F_{sim}$  for sampling cloth parameters for each episode during training. Visual properties such as lighting, noise in image observations and camera position are also sampled for each episode from a uniform distribution with empirically chosen ranges.

The second main element of our method that facilitates a zero-shot transfer is employing the controller of the real manipulator in the policy learning process. For performing cloth manipulation in the real world we use a cascaded structure combining a low-frequency policy with a Cartesian controller operating at a high-frequency required by the real hardware. The Cartesian controller maps the desired positions of the end-effector given by the policy into the desired joint torques of the robotic manipulator. In this work, we use Operational Space Control (OSC) as the Cartesian controller. We use the same Cartesian controller in the simulated and real environments, which enables transferring the policies in a zero-shot manner. The gains of the Cartesian controller are not tuned to a specific task prior to training, but we instead let the policy implicitly learn the dynamics of the controller during training. To be able to provide a continuous reference signal to the OSC controller in between policy steps, the desired end-effector position is interpolated  $K$  times from  $\mathbf{x}_t$  to  $\mathbf{x}_{t+1}$  according to

$$\mathbf{x}_{t,j+1} = 0.03 \cdot (\mathbf{x}_t + \mathbf{a}_t) + 0.97 \cdot \mathbf{x}_{t,j}, \quad (3)$$

where  $\mathbf{x}_{t,0}$  is the initial end-effector position and  $\mathbf{x}_t + \mathbf{a}_t$  is the target end-effector position.

## V. EXPERIMENTS

The goal of the experiments is to evaluate the proposed method in dynamic cloth manipulation against baselines that a) do not use visual feedback and b) use visual feedback but do not apply cloth dynamics randomization during training. To compare the proposed method against the baselines, we design a dynamic sideways folding task and compare the accuracy of the methods both in simulation and the real world.

### A. Dynamic sideways cloth folding task

The dynamic sideways folding task requires manipulating flat cloths into a folded configuration, where only a single point of the cloth can be controlled. The starting and folded states are shown on the left and right sides of Fig. 3 respectively. We consider  $C = 8$  cloth points ( $\mathbf{p}_i, \mathbf{g}_i$ ), where  $\mathbf{p}_1$  is the only grasped-corner. The task requires manipulating  $\mathbf{p}_1$  so that both  $\mathbf{p}_1$  and  $\mathbf{p}_0$  move from their initial positions to the desired goal locations  $\mathbf{g}_1$  and  $\mathbf{g}_0$ . For a fold to be considered successful, the distance  $d_i = \|\mathbf{p}_i - \mathbf{g}_i\|_2$  should be below a threshold  $\delta = 4$  cm for the corners ( $i \in \{0, 1\}$ ) at the end of an episode. If the fold is considered to be successful, the reward is dispensed at each time step according to

$$r_t = \frac{1}{2} \sum_{i=0}^1 \frac{\|\mathbf{p}_i - \mathbf{g}_i\|_2}{\delta}, \quad (4)$$

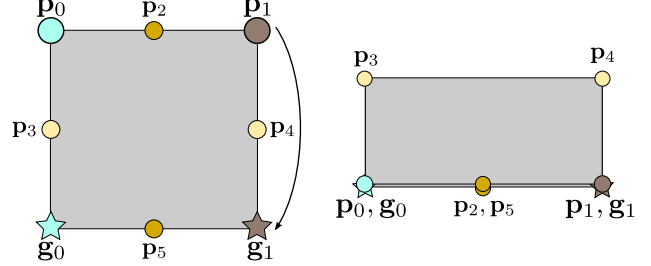


Fig. 3: Start (left) and desired (right) end configurations of the cloth for the dynamic sideways folding task, where  $\mathbf{p}_1$  is the only grasped-corner,  $\mathbf{p}_0$  is one of the non-grasped corner, and  $\mathbf{g}_1, \mathbf{g}_0$  their respective goal locations.

where the reward scales linearly from 0 to 1 based on the distances  $d_i$ . If the task is considered unsuccessful, then the reward is  $-1$ .

In this task, the agent observes  $100 \times 100$  pixel grayscale images  $\mathcal{I}$  taken from the side of the cloth and maps them into continuous actions as specified in Section IV-B. For the sideways folding task, the actions are scaled to a range of  $[-0.03, 0.03]$  for each dimension, that represent the desired change of the end-effector (in cm) position in Cartesian coordinates.

### B. Baselines

The proposed method ( $\pi_{ours}$ ) uses visual feedback and cloth parameter randomization to solve the defined sideways folding task. The task definition and the demonstration based cloth parameter identification scheme defined in Section IV-B are used to find  $M = 20$  sets of cloth parameters that are randomly sampled during training to be used in the experiments.

The first method we use as a baseline to compare against the proposed method is based on Jangir *et al.* [8], which we denote as  $\pi_{fixed}$ , where a policy directly observes the cloth positions and velocities ( $\mathbf{p}_i, \dot{\mathbf{p}}_i$ ) instead of an image  $\mathcal{I}$  during training. Only a single set of parameters  $\theta_c$  are used during training, and the selection is made based on the largest achieved rewards at the end of an episode found during cloth parameter identification. Policies trained with this baseline are not directly transferable to the real world since the cloth internal states are not available. Therefore, only fixed trajectories from simulation are evaluated on the real hardware. Compared to the method in [8], we use SAC instead of Deep Deterministic Policy Gradient (DDPG) [22] for training  $\pi_{fixed}$ .

The second baseline ( $\pi_{ours-}$ ) is identical to the proposed method, except it only uses a single set of cloth dynamics parameters in training, where the cloth parameters  $\theta_c$  are chosen similarly to  $\pi_{fixed}$ . The policy  $\pi_{ours-}$  serves a baseline of the proposed method to provide evidence of the benefits of randomizing the cloth dynamics during the policy training phase.

TABLE I: Fabric types  $F_{real}$  used in the real world experiments.

Cloth	Fabric type	Weight (g/m <sup>2</sup> )
Orange	Polyester	135
White	Cotton	345
Blue	Cotton	400

### C. Simulation setup and training

The simulated environment is implemented in MuJoCo [23] where a model of the Franka Emika Panda [24] is included along with the 2D grid of bodies representing the cloth. The environment episode has a length of 25 policy time steps. The simulation itself is stepped 10 times between each policy step where each simulation step is 10 milliseconds long. An episode is also terminated if the end-effector/corner  $\mathbf{p}_1$  is within  $\delta = 4\text{cm}$  from its goal for more than 10 policy time steps. At each training episode the cloth goal corner  $\mathbf{g}_i$  is sampled within 2cm of the adjacent corners to  $\mathbf{p}_0$  and  $\mathbf{p}_1$ .

The policy training is performed for 100 epochs, where each epoch consists of 20 cycles of 1000 environment time steps. At the end of each cycle, the collected observations are added into a replay buffer and policy optimization is performed for 1000 gradient steps using SAC. Each epoch is concluded with 20 evaluation episodes where the success rate and corner distances to the goals are measured.

### D. Real world setup

The real world experiments are performed using the Franka Emika Panda robot and the Robot Operating System [25]. To capture visual feedback for the policies  $\pi_{ours-}$  and  $\pi_{ours}$ , we use an Intel RealSense D435 depth camera, where we use only the infrared modality to reduce the latency [26]. The auxiliary corner predictions from the policies  $(\mathbf{u}, \mathbf{v})$  (see Fig 2) are used to tune the exact camera position prior to executing the policies. The corner predictions act as a measurement of how well the policy predictions align between the simulated and real environments.

In order to validate the performance over different cloth types (Table I), the real world experiments are run with 3 different test cloths  $F_{real} = \{f_{orange}, f_{white}, f_{blue}\}$ . The cloths properties can be qualitatively differentiated as  $f_{blue}$  the most rigid and  $f_{orange}$  as the most shallow and susceptible to more deformation when manipulated.

The policies to be evaluated in the real world were picked from the epochs where the maximum success rate was achieved (Section VI-A). Each method is evaluated for 10 episodes on all of the cloth types, resulting in a total of 90 different trajectories. Prior to running an evaluation, the cloth to be folded is attached to the robot end-effector and the robot is reset to the same joint configuration for each episode. The same grasping and camera configuration in addition to lighting conditions are kept fixed across all evaluation types to make the evaluation as standardized as possible. The evaluation includes empirically measuring the distance

of  $\mathbf{p}_0$  and  $\mathbf{p}_1$  to their goal locations  $\mathbf{g}_0$  and  $\mathbf{g}_1$  at the end of the trajectory. The goals  $\mathbf{g}$  are provided to the policies based on the cloth sizes, as the desired positions of the adjacent corners relative to the end-effector are known and kept fixed during the evaluation. Each trajectory ends after 25 policy steps, or if the end-effector has been within  $\delta = 4\text{cm}$  of the goal corner as in the simulated setup.

## VI. RESULTS

We evaluate the folding performance of the different policies by measuring the sum of the distances of the grasped and non-grasped corners to their goals  $d_{sum} = \sum_{i=0}^{0,1} \|\mathbf{p}_i - \mathbf{g}_i\|_2$  once each trajectory has finished. It should be noted that  $d_{sum}$  was used in the reward function during training so measuring it serves to assess Sim2Real transfer quality. To determine whether any difference in the evaluation metrics between the methods are statistically significant we use the Mann-Whitney U test for the real world experiments (Section VI-B). We choose a statistical significance level of 0.05 prior to the evaluations to assess whether the underlying distributions of the corner distance measurements across evaluations differ at least by the amount reported.

### A. Simulation results

First, to set a baseline for the real world folding task, we assess the performance of the policy evaluation during training over five different random seeds via the metric  $d_{sum}$  (Fig. 4), along with the success rate (Fig. 6) for each method.

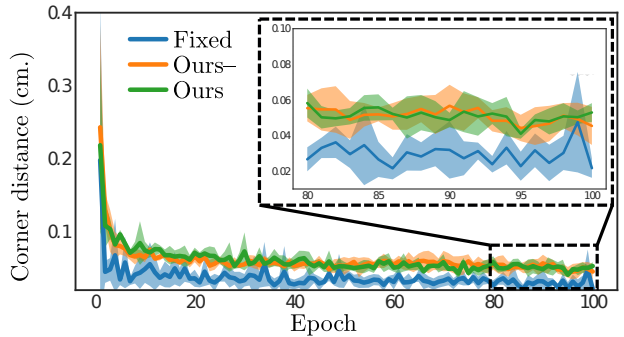


Fig. 4: Mean and standard deviation of the **error**  $d_{sum}$  (in cm) for each evaluation epoch during training in simulation for each method.

The simulation results show that the task can be learned by all the methods within 100 epochs. The fixed policy based on the work by Jangir *et al.* [8] is able to learn the task only after a few epochs. We hypothesize that the success rate converges faster than in what is reported by [8] due to the fact that we omit the grasping problem. Additionally, the use of SAC is expected to aid in exploration compared to DDPG used by [8]. The corner distances  $d_{sum}$  achieved by  $\pi_{fixed}$  ranges from 2-4 cm on average at the end of training, which is approximately 50% less than the visual feedback-based methods. This result suggests that observing the exact positions and velocities of selected points on the cloth can attain more accurate folds than the visual observations of our method.

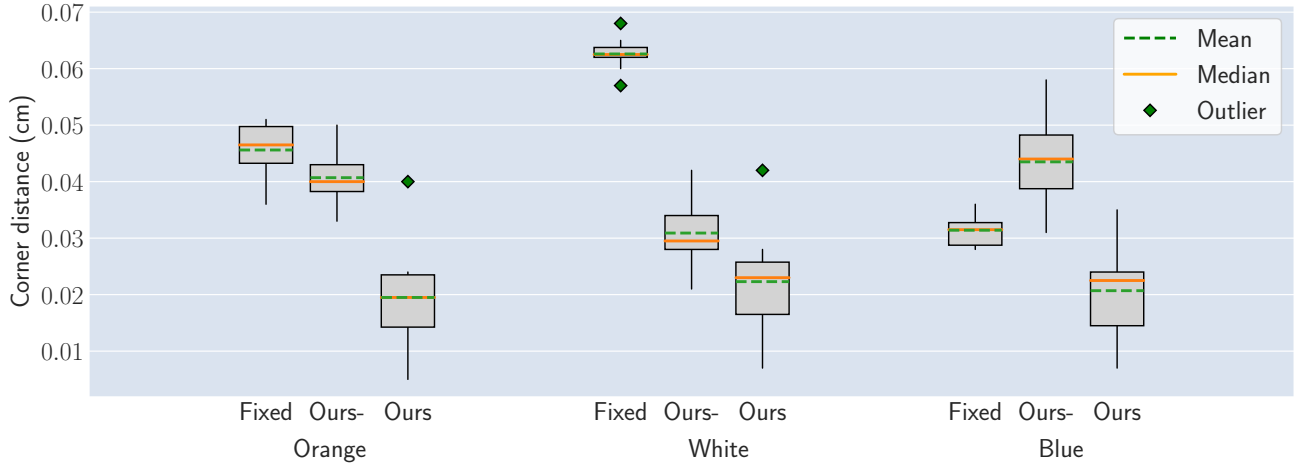


Fig. 5: Real world measurements of corner distance errors  $d_{\text{sum}}$  (in cm) for the different methods.

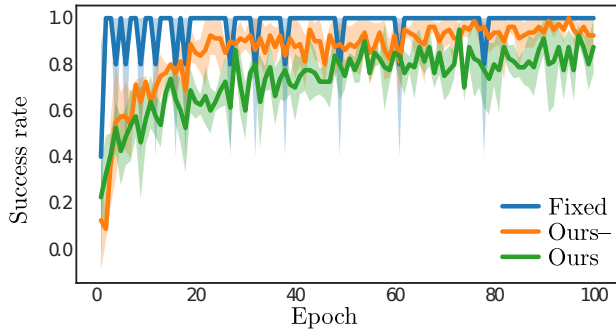


Fig. 6: Mean **success rate** and variance for each evaluation epoch during training for each method.

### B. Real world results

We provide the real world error metric  $d_{\text{sum}}$  for each fabric and evaluation type on Fig. 5. The first thing to note is that the proposed method  $\pi_{\text{ours}}$  significantly outperforms the other methods consistently for all cloth types, and the achieved error  $d_{\text{sum}}$  even falls below the range seen during simulation training. For the fixed trajectories from  $\pi_{\text{fixed}}$ , the error is significantly higher in the real world for all the cloth types compared to simulation, which highlights the Sim2Real gap. Moreover, the fact that the cloth dynamics are different can be seen from the variability across the different cloth types. The visual feedback-based method  $\pi_{\text{ours-}}$  performs considerably better compared to trajectories from  $\pi_{\text{fixed}}$  for the white cloth, but is comparable or worse for the other cloth types, again highlighting the differences in cloth dynamics.

The variance of  $d_{\text{sum}}$  for both  $\pi_{\text{ours-}}$  and  $\pi_{\text{ours}}$  compared to the fixed trajectory from  $\pi_{\text{fixed}}$  shows that the results produced by the feedback-based methods are less stable. This points to the fact that the policies are susceptible to noise from the environment such as lighting and camera movement, as well as the noise due to the subtle differences in starting configuration that also affects the fixed trajectories. Comparing  $d_{\text{sum}}$  of the proposed method to  $d_{\text{sum}}$  of the baselines

shows statistical significance for all cloth types, as shown in Table II.

TABLE II: Statistical significance (p-values) of differences between Ours against the evaluated baseline methods using the Mann-Whitney U test. All results are statistically significant ( $p < 0.05$ ).

	Fixed	Ours-
Ours (Orange)	$4 \cdot 10^{-5}$	$2 \cdot 10^{-4}$
Ours (White)	$1 \cdot 10^{-5}$	$9 \cdot 10^{-3}$
Ours (Blue)	$2 \cdot 10^{-3}$	$4 \cdot 10^{-5}$

To evaluate how the feedback-based policies react to feedback and noise from the environment, we show the end-effector trajectories for each fabric and policy in Fig. 7. The trajectories for  $\pi_{\text{fixed}}$  are nearly identical since the same exact trajectory is executed for each fabric type. On the other hand, trajectories from  $\pi_{\text{ours-}}$  present a minor deviation for different cloth types. We hypothesize that the policy has learned to approximately memorize a certain trajectory for the single cloth type it was trained for, based on the goal and previous actions, and it only reacts mildly to the feedback of the differing cloth types. The trajectories from  $\pi_{\text{ours}}$  showcase more variation over the different fabric types and it can be observed that the trajectories differ more towards the end of the manipulation, which points to the fact that the policy gains enough information about a certain cloth type after a certain amount of time steps. We hypothesize that only quasi-static forces affect the manipulation early on in the trajectory, which allows the different cloths to be manipulated with a similar movement. However, after forces due to acceleration come into play (non-manipulated corner falls due to gravity), the policy needs to react to the different dynamic behavior across cloths. This result is consistent with the findings in Fig. 5, where  $\pi_{\text{ours}}$  was capable to adjust to the different cloth types as opposed to the other methods.

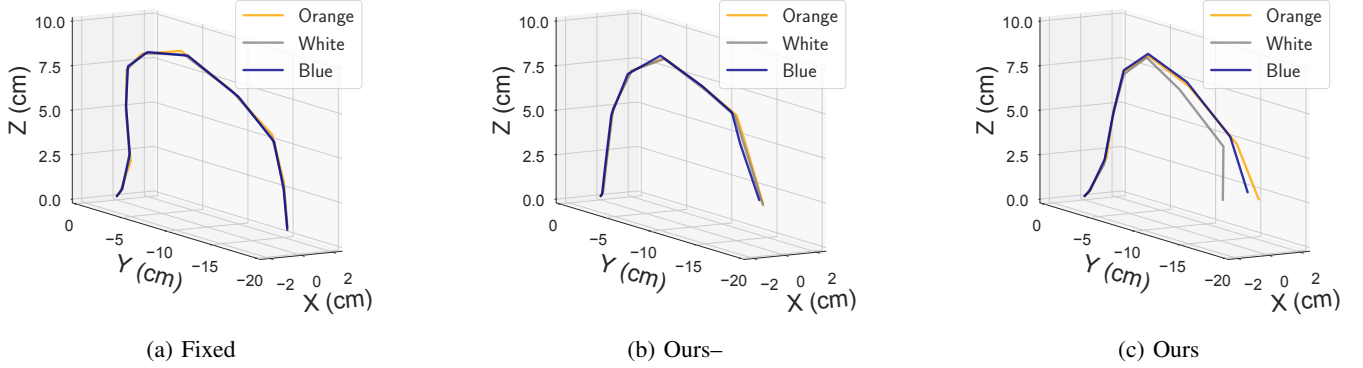


Fig. 7: Mean of trajectories from real world experiments on the three fabric types for all compared methods.

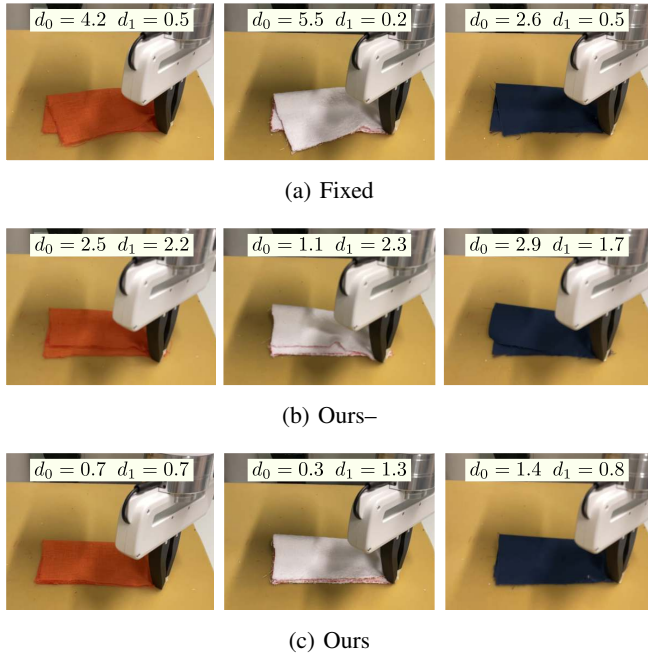


Fig. 8: Qualitative and quantitative results showing the end configurations for each cloth type after a fold for each policy, where  $d_0$  and  $d_1$  represent the distance to the left and right corners respectively.

Qualitatively,  $\pi_{\text{ours}}$  achieves the most consistent folds compared to the other methods across all the different cloth types as shown in Fig. 8. On the other hand, fixed trajectories from  $\pi_{\text{fixed}}$  and the trajectories from  $\pi_{\text{ours-}}$  fail to achieve a perfect fold. For  $\pi_{\text{fixed}}$ , the orange (lightest) and the blue (heaviest) cloths produce better folds than the white cloth, hinting that the dynamics are affected by not only the fabric weight but other features as well. The qualitative results further support the quantitative results where the fixed trajectory did not produce similar errors  $d_{\text{sum}}$  for all cloth types. The trajectories achieve folds where the non-grasped corner reaches past its goal, possibly meaning that the cloth used in the simulation is less rigid than any of the tested real cloths  $F_{\text{real}}$ . Since the trajectories executed by  $\pi_{\text{ours-}}$  only differ slightly for each fabric, it is not surprising that the qualitative

folds are not perfect. Instead of the non-grasped corner going past its goal, it usually does not reach the desired goal. We attribute the superior performance of  $\pi_{\text{ours}}$  compared to the baselines to its better ability to react to feedback compared to  $\pi_{\text{ours-}}$  as also shown in Fig. 5 and Fig. 7.

As a conclusion, we provide evidence that randomizing cloth parameters in simulation enables the policy to account for different dynamical behavior of different materials. The fact that  $\pi_{\text{ours-}}$  is not able to generalize to different fabrics is expected since it is limited to a single type of cloth during training.

## VII. CONCLUSION

We presented a visual feedback-based solution for dynamic cloth manipulation in the real world. The method uses Reinforcement Learning and a simulated environment to allow training cloth manipulation policies in simulation and transferring it to the real world. We showed that our method successfully trains policies that are able to successfully perform dynamic cloth manipulation in the real world and generalize across different materials. We provided experimental results showing that using visual feedback improves folding performance compared to predefined folding trajectories across different materials. We also provided evidence that randomizing the cloth dynamics in simulation is essential for making the policy capable to react to feedback from different types of materials. The main limitations of this work are that the proposed method only considers fixed-size pieces of cloth and that the cloth grasping problem is considered solved.

Considerations for future work based on this paper are two-fold. First, future work in dynamic cloth folding should further explore finding policies that work on a larger range of different cloths (size, dynamics) as well as more challenging real world contexts where it is not reasonable to assume a successful grasp beforehand. Secondly, in order to move further towards general solutions for cloth manipulation such as bed-making and folding clothes on a larger scale, simulators with higher fidelity should be developed. As the manipulated cloths get more complex, it is hard to see that the use of simulated environments would be decreasing.

## REFERENCES

- [1] S. Miller, J. Van Den Berg, M. Fritz, T. Darrell, K. Goldberg, and P. Abbeel, “A geometric approach to robotic laundry folding,” *The International Journal of Robotics Research*, vol. 31, no. 2, pp. 249–267, 2012.
- [2] D. Seita, N. Jamali, M. Laskey, A. K. Tanwani, R. Berenstein, P. Baskaran, S. Iba, J. Canny, and K. Goldberg, “Deep transfer learning of pick points on fabric for robot bed-making,” *arXiv preprint arXiv:1809.09810*, 2018.
- [3] Y. Gao, H. J. Chang, and Y. Demiris, “Iterative path optimisation for personalised dressing assistance using vision and force information,” in *2016 IEEE/RSJ international conference on intelligent robots and systems (IROS)*. IEEE, 2016, pp. 4398–4403.
- [4] G. Canal, E. Pignat, G. Alenyà, S. Calinon, and C. Torras, “Joining high-level symbolic planning with low-level motion primitives in adaptive hri: Application to dressing assistance,” in *2018 IEEE International Conference on Robotics and Automation (ICRA)*. IEEE, 2018, pp. 3273–3278.
- [5] M. Mason and K. Lynch, “Dynamic manipulation,” in *Proceedings of 1993 IEEE/RSJ International Conference on Intelligent Robots and Systems (IROS '93)*, vol. 1, 1993, pp. 152–159 vol.1.
- [6] J. Matas, S. James, and A. J. Davison, “Sim-to-real reinforcement learning for deformable object manipulation,” *arXiv preprint arXiv:1806.07851*, 2018.
- [7] B. Balaguer and S. Carpin, “Combining imitation and reinforcement learning to fold deformable planar objects,” in *2011 IEEE/RSJ International Conference on Intelligent Robots and Systems*. IEEE, 2011, pp. 1405–1412.
- [8] R. Jangir, G. Alenyà, and C. Torras, “Dynamic cloth manipulation with deep reinforcement learning,” *arXiv preprint arXiv:1910.14475*, 2019.
- [9] H. Ha and S. Song, “Flingbot: The unreasonable effectiveness of dynamic manipulation for cloth unfolding,” *arXiv preprint arXiv:2105.03655*, 2021.
- [10] J. Maitin-Shepard, M. Cusumano-Towner, J. Lei, and P. Abbeel, “Cloth grasp point detection based on multiple-view geometric cues with application to robotic towel folding,” in *2010 IEEE International Conference on Robotics and Automation*. IEEE, 2010, pp. 2308–2315.
- [11] B. Willimon, S. Birchfield, and I. Walker, “Model for unfolding laundry using interactive perception,” in *2011 IEEE/RSJ International Conference on Intelligent Robots and Systems*. IEEE, 2011, pp. 4871–4876.
- [12] L. Sun, G. Aragon-Camarasa, P. Cockshott, S. Rogers, and J. Paul, “A heuristic-based approach for flattening wrinkled clothes.”
- [13] H. Yuba, S. Arnold, and K. Yamazaki, “Unfolding of a rectangular cloth from unarranged starting shapes by a dual-armed robot with a mechanism for managing recognition error and uncertainty,” *Advanced Robotics*, vol. 31, no. 10, pp. 544–556, 2017.
- [14] D. Triantafyllou, I. Mariolis, A. Kargakos, S. Malassiotis, and N. Aspragathos, “A geometric approach to robotic unfolding of garments,” *Robotics and Autonomous Systems*, vol. 75, pp. 233–243, 2016.
- [15] Y. Wu, W. Yan, T. Kurutach, L. Pinto, and P. Abbeel, “Learning to manipulate deformable objects without demonstrations,” *arXiv preprint arXiv:1910.13439*, 2019.
- [16] D. Seita, A. Ganapathi, R. Hoque, M. Hwang, E. Cen, A. K. Tanwani, A. Balakrishna, B. Thananjeyan, J. Ichnowski, N. Jamali, *et al.*, “Deep imitation learning of sequential fabric smoothing from an algorithmic supervisor,” in *2020 IEEE/RSJ International Conference on Intelligent Robots and Systems (IROS)*. IEEE, 2020, pp. 9651–9658.
- [17] R. Hoque, D. Seita, A. Balakrishna, A. Ganapathi, A. K. Tanwani, N. Jamali, K. Yamane, S. Iba, and K. Goldberg, “Visuospatial foresight for multi-step, multi-task fabric manipulation,” *arXiv preprint arXiv:2003.09044*, 2020.
- [18] A. Ganapathi, P. Sundaresan, B. Thananjeyan, A. Balakrishna, D. Seita, J. Grannen, M. Hwang, R. Hoque, J. E. Gonzalez, N. Jamali, *et al.*, “Learning dense visual correspondences in simulation to smooth and fold real fabrics,” *arXiv preprint arXiv:2003.12698*, 2020.
- [19] O. Khatib, “A unified approach for motion and force control of robot manipulators: The operational space formulation,” *IEEE Journal on Robotics and Automation*, vol. 3, no. 1, pp. 43–53, 1987.
- [20] T. Haarnoja, A. Zhou, P. Abbeel, and S. Levine, “Soft actor-critic: Off-policy maximum entropy deep reinforcement learning with a stochastic actor,” in *International Conference on Machine Learning*. PMLR, 2018, pp. 1861–1870.
- [21] M. Andrychowicz, F. Wolski, A. Ray, J. Schneider, R. Fong, P. Welinder, B. McGrew, J. Tobin, P. Abbeel, and W. Zaremba, “Hindsight experience replay,” *arXiv preprint arXiv:1707.01495*, 2017.
- [22] T. P. Lillicrap, J. J. Hunt, A. Pritzel, N. Heess, T. Erez, Y. Tassa, D. Silver, and D. Wierstra, “Continuous control with deep reinforcement learning,” *arXiv preprint arXiv:1509.02971*, 2015.
- [23] E. Todorov, T. Erez, and Y. Tassa, “Mujoco: A physics engine for model-based control,” in *IROS*. IEEE, 2012, pp. 5026–5033. [Online]. Available: <http://dblp.uni-trier.de/db/conf/iros/iros2012.html#TodorovET12>
- [24] F. E. GmbH. [Online]. Available: <https://www.franka.de/technology>
- [25] Stanford Artificial Intelligence Laboratory *et al.*, “Robotic operating system.” [Online]. Available: <https://www.ros.org>
- [26] “High-speed capture mode of intel® realsense™ depth camera d435.” [Online]. Available: <https://dev.intelrealsense.com/docs/high-speed-capture-mode-of-intel-realsense-depth-camera-d435>